© Universiti Tun Hussein Onn Malaysia Publisher's Office

IJIE

http://penerbit.uthm.edu.my/ojs/index.php/ijie
ISSN : 2229-838X e-ISSN : 2600-7916

The International Journal of Integrated Engineering

Application of Foamed Concrete and Cold-Formed Steel Decking as Lightweight Composite Slabs: Experimental Study On Structural Behaviour

Z. M. Jaini[1, 2*], R. H. M. Rum[3], S. J. Seyed Hakim[2], S. N. Mokhatar[2]

[1]Structures Management Engineering, Graduate School of Engineering, Kyoto University, Kyoto 615-8540, JAPAN

[2]Structural Dynamics and Computational Engineering, Faculty of Civil Engineering and Built Environment, Universiti Tun Hussein Onn Malaysia, 86400 Parit Raja, Johor, MALAYSIA

[3]Johor Federal Project Implementation Unit, Department of Irrigation and Drainage, 79626 Iskandar Puteri, Johor, MALAYSIA

*Corresponding Author

DOI: https://doi.org/10.30880/ijie.2023.15.02.009
Received 20 February 2023; Accepted 10 May 2023; Available online 31 July 2023

Abstract: This paper presents an investigation of ultimate load, maximum deflection and failure mode of foamed concrete composite slabs (FCCS). Of interest are the effects of dry density and slab thickness. Unlike conventional composite slabs, FCCS has the advantage of eliminating the selfweight penalty and thus reducing the underlying structural members. With the advanced research in concrete technology, foamed concrete with sufficient strength properties to meet the requirements of standard code of practise has been successfully introduced. Foamed concrete is known for its lightweight and versatility. In the experimental study, the slab specimens with a span of 1800 mm, a width of 840 mm and different slab thicknesses of 100 mm to 150 mm were prepared for the three-point bending test. The dry density of foamed concrete is 1400 kg/m^3, 1600 kg/m^3, and 1800 kg/m^3, which has a compressive strength of about 20 MPa to 40 MPa. Dry density and slab thickness have been observed to have significant effects on ultimate load and maximum deflection. Higher dry density of foamed concrete provides better slip resistance and thus reduces shear bond failure. On the other hand, slab specimens with a higher slab thickness tend to have better bearing capacity due to greater bending stiffness. The main failure mode is dominated by localised bending on the profiled steel deck, slip-displacement and fracture of the foamed concrete.

Keywords: Lightweight composite slabs, foamed concrete, profiled steel deck, ultimate load, maximum deflection, localised bending, slip-displacement, fracture

1. Introduction

Engineered specifically for flooring systems, composite slabs offer good durability properties and are an efficient replacement for reinforced concrete slabs. BS EN 1994-1-1 [1] defines composite slabs as a method of construction where a profiled steel deck is used first as permanent formwork, then structurally connected to the concrete and acts as tensile reinforcement. The profiled steel deck serves not only as permanent formwork for the concrete, but also provides a shear connection mechanism once the concrete has hardened. The impressive fact is that composite slabs can speed up the construction process. According to Rackham et al. [2], the use of composite slabs in buildings is a safe approach and economical. Composite slabs are considered to be one of the best diaphragm-strengthening techniques, allowing for

**Corresponding author: rizuan@uthm.edu.my*

higher bearing capacity, lower slab thickness and a reduction in the size of the underlying structural members [3]. Composite slabs are currently mostly cast from normal concrete. A major concern, however, is the selfweight penalty of normal concrete which contributes a large portion to permanent action. Therefore, Martinez-Martinez et al. [4], Jayaseelan et al. [5], Dian-Zhong & Shi-Hao [6], Lv et al. [7] and many others proposed the use of lightweight concrete to address this issue. Lightweight concrete has a lower density and is typically 35% lighter than normal concrete.

At present, the use of lightweight concrete as load-bearing structures is subjected to some limitations due to poor strength properties. Zhang [8], Hedjazi [9] and Chaipanich & Chindaprasirt [10] stated that lightweight concrete should have adequate compressive strength in the range of 15 MPa. However, for load-bearing structures, BS EN 1992-1-1 [11] stipulates that the minimum compressive strength shall not be less than 22 MPa. While ASTM C330 [12] allows the use of lightweight concrete with a minimum compressive strength of 17 MPa, it is always preferable to choose lightweight concrete with higher compressive strength. The success in developing lightweight concrete with sufficient strength properties by Hamad [13], Evangelista & Tam [14], Hung et al. [15], Liu et al. [16] and Ibrahim et al. [17] or exceptionally ultra-high performance by Lu et al. [18], Pan et al. [19] and Alanazi et al. [20] have paved the way for the application of lightweight concrete to composite slabs. The use of lightweight concrete is also motivated by the trend towards green and environmental sustainability. In addition, lightweight concrete is a viable alternative to normal concrete and can be produced to a desired density. The choice of lightweight concrete is very diverse, including lightweight aggregate concrete, foamed concrete, no-fines concrete and ultra-lightweight concrete.

This paper examines the potential of foamed concrete for lightweight composite slabs. Of interest are the effects of dry density and slab thickness on structural behaviour in terms of ultimate load, maximum deflection and failure mode. Despite many advantages that foamed concrete offers, there are some disadvantages that currently constrain its application as structural elements. Shear provision design, for example, lags far behind normal concrete. Furthermore, the bond strength that control bearing capacity is not well understood. In the case of lightweight composite slabs, the bearing capacity is governed by the strength properties, in particular the compressive strength. For foamed concrete, the compressive strength depends too much on the dry density. On the other hand, the slab thickness plays a decisive role in determining the bending stiffness. It is therefore worth conducting an investigation into the effects of dry density and slab thickness. Lightweight composite slabs made of foamed concrete and profiled steel deck, hereinafter referred to as foamed concrete composite slabs (FCCS), are attractive and conform to the standard of industrialized building systems. FCCS is intended to become an ideal solution to the selfweight penalty and subsequently promote optimal construction costs.

2. Lightweight Composite Slabs

Whether for renovation/refurbishment or adding a storey (increasing the height of a building), the construction of lightweight composite slabs offers many benefits. According to Luu et al. [21], the use of lightweight composite slabs reduced structural loads by up to 40%. This is particularly useful for minimizing the need for underpinning existing frames and preventing overloading at the tops of buildings in seismic zones. Moreover, the combination of lower selfweight and higher strength allows greater freedom of design and opportunities for architectural expression, especially for commercial and industrial buildings. Previous researchers such as Alvarez Rabanal et al. [22], Bruedern at el. [23] and Yankun et al. [24] utilized lightweight aggregate concrete as a topping material for lightweight composite slabs. Lightweight aggregate concrete can be produced like normal concrete to meet the required strength properties. The difference is that fly ash ceramisite, slag ball, cinder, expanded clay and expanded perlite can be used to replace natural aggregates. The use of lightweight aggregate concrete has been found reducing the bearing capacity of lightweight composite slabs by between 11% to 25% compared to conventional composite slabs. The main failure mode is dominated by shear bond failure.

An investigation by Flores-Jonshon & Li [25] was carried out for lightweight composite slabs made of foamed concrete and profiled steel deck. To observe the structural behaviour, the lightweight composite slabs were subjected to the four-point bending test. Instead of the topping material, foamed concrete was used as the core material. There are two types of foamed concrete used in the preparation of lightweight composite slabs, plain foamed concrete and fibrous foamed concrete. The density of foamed concrete is kept constant at almost 1000 kg/m^3. The compressive strength of plain foamed concrete is 4.78 MPa, while the compressive strength of fibrous foamed concrete is 8.83 MPa. Despite the lower compressive strength, the peak breaking load reaches 19.49 kN and 38.65 kN for the lightweight composite slabs with plain foamed concrete and fibrous foamed concrete, respectively. The deflection of the lower top surface was recorded during the peak breaking load, and the value ranged from about 2.67 mm to 5.36 mm. On the other hand, Low et al. [26] proposed the use of foamed concrete on lightweight composite slabs for floating floor systems. The lightweight composite slabs were examined to obtain the failure mechanism under full load capacity. In another study by Sutiman et al. [27], foamed concrete was used as the infill material for the lightweight composite slabs, which consist of Prima*flex* dry board and PEVA 50. It was found that foamed concrete has a minor impact on serviceability.

Sohel et al. [28] investigated the bond-slip behaviour of lightweight composite slabs made of ultra-lightweight concrete and profiled steel deck. The density of ultra-lightweight concrete is 1440 kg/m^3. The bond strength determined from the experimental study was compared to that of conventional composite slabs at short and long spans. It was observed that the lightweight composite slabs exhibited higher ductile behaviour and higher bearing capacity. In terms of bond strength, there is an insignificant difference between lightweight composite slabs and conventional composite slabs. A nonlinear thermos-structural analysis by Martinez-Martinez [4] showed that lightweight composite slabs do not meet the minimum bearing capacity of 30 minutes required by BS EN 1994-1-2 [29]. The lightweight concrete was produced from siliceous aggregates and expanded clay, and achieves a compressive strength of around 25 MPa to 30 MPa. Despite existing of embossments, there are still detachments between the lightweight concrete and the profiled steel deck. This phenomenon occurs because the lightweight concrete and the profiled steel deck have different rates of thermal expansion. The maximum deflection of lightweight composite slabs, especially those made of lightweight concrete with lower density, exceeded the serviceability criterion.

3. Experimental Study

3.1 Preparation of Foamed Concrete

Casting FCCS requires preparation of foamed concrete and profiled steel deck. For foamed concrete, the basic materials include Ordinary Portland cement (OPC), sand and water. In this experimental study, OPC is used due to accessible resources. This type of cement is known for its excellent binding properties that provide structural members with sufficient strength properties. Meanwhile, sand was sieved to a fine size of about 3 mm. According to BS EN 12620 [30], the size distribution of sand must be uniform to ensure the quality of the concrete mix. BS EN 1008 [31] requires water to be free of impurities to avoid contamination on the protein of foaming agent which can affect the quality of the concrete mix. Unlike normal concrete, foamed concrete does not require coarse aggregate. Therefore, foamed concrete can maintain its lower density. In addition to the basic materials, foamed concrete requires additive materials such as foaming agent, superplasticizer, rice husk ash (RHA) and polypropylene mega-mesh (PMM). Fig. 1 shows the basic and additive materials used to produce foamed concrete. Foaming agent is a crucial substance to create air contents in foamed concrete. In this experimental study, Sika AER 50/50 was used as the foaming agent due to its highly concentrated liquid admixture and its stable chemical components which allows the generation of consistent air contents.

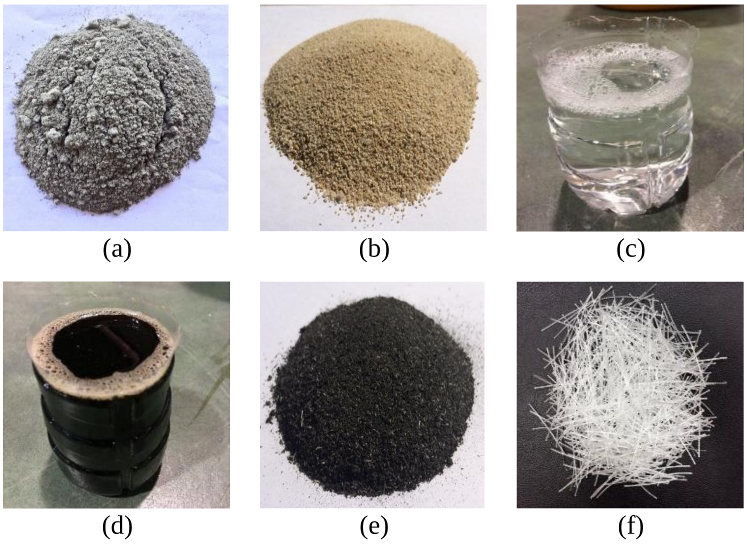

Fig. 1 - Basic and additive materials used to produce foamed concrete; (a) OPC; (b) sand; (c) foaming agent; (d) superplasticizers; (e) RHA; (f) PMM

The incorporation of superplasticizer into foamed concrete shall be managed in accordance with BS EN 934-2 [32]. ESTOP Admix AP was used to achieve better workability of the concrete mix. The presence of RHA and PMM causes the concrete mix to become too viscous. It is, therefore, necessary to add superplasticizer to the concrete mix. RHA is used as a partial sand replacement in the range of up to 40%. This type of agricultural waste comes from Muar Rice Factory, Johor. The colour is a mixture of black and white resulting from uncontrolled burning below 700°C for 6 hours. RHA contains pozzolanic substances that help improve cementitious properties. PMM as fibre reinforcement has a length of 55 mm with mechanical properties of 0.9 kg/dm^3 specific gravity, 7.289 GPa modulus of elasticity and 425 MPa tensile strength. PMM is based on homo-polypropylene (micro-synthetics fibre) with a chemical composition of 33% carbon and 67% hydrogen. Besides its roles as fibre reinforcement, PMM also acts as a filler for the cavities created by the air voids. Jaini et al. [33] suggested that the maximum dosage of PMM is 9 kg/m^3. Beyond this dosage, PMM will reduces the compressive strength. PMM was found to be able to disrupt the cohesion of dry microstructures and cause the air contents collapse easily.

3.2 Mix Design

As foamed concrete is intended for use in lightweight composite slabs, BS EN 1992-1-1 [11] specifies that the compressive strength should not be less than 22 MPa. In general, the compressive strength of foamed concrete is determined by its density and depends on the amount of foam added to the concrete mix. Plain foamed concrete rarely achieves a compressive strength of more than 15 MPa, which is usually only suitable for non-structural purposes [34], [35]. The addition of additive materials such as silica fume, fly ash and steel fibres to foamed concrete greatly improves compressive strength. With that condition, a provision of mix design is necessary. Previous researchers such as Othman et al. [36], Al Qubro et al. [37], Ma et al. [38] and Guo et al. [39] successfully developed the mix design of foamed concrete with the inclusion of additive materials. Since this experimental study intends to use RHA and PMM, the mix design proposed by Abd Rahman et al. [40] was found suitable and thus adopted. Table 1 shows the detailed of mix design. For the dry density range from 1400 kg/m^3 to 1800 kg/m^3, the mix design remains similar but the amount of foam was manually adjusted to the desired density. It should be noted that the content of superplasticizer added to the concrete mix is proportional to the weight of the cement.

Table 1 - Mix design of foamed concrete

Density (kg/m^3)	S:RHA (%)	PMM (kg/m^3)	W/C Ratio	C/S Ratio	FA/C Ratio	FA/W Ratio	SP (%)
1400							
1600	60:40	9	0.55	0.50	0.70	0.05	0.55
1800							

Note: RHA = Rice husk ash, PMM = Polypropylene mega-mesh
S = Sand, W = Water, C = Cement, FA = Foaming agent, SP = Superplasticizer

3.3 Specimens

Cube specimens were cast using 100 mm × 100 mm × 100 mm moulds. This is a standard size for concrete without coarse aggregate and is compatible with foamed concrete as used by Wong et al. [41], Gołaszewski et al. [42], Shawnim & Mohammad [43], Chen & Yu [44] and Ouédraogo et al. [45]. Table 2 shows the number of cube specimens. Cube specimens were subjected to an air curing process at ambient temperature for 7, 14 and 28 days. Meanwhile, slab specimens were cast based on the required dimensions to BS EN 1992-1-1 [11]. The span (L) is 1800 mm and width (w) is 840 mm. The slab thickness (h) is 100 mm, 125 mm and 150 mm. The profile depth (h_s) remains constant at 45 mm. Thus, the thickness of above the main flat surface (h_c) corresponds to 55 mm, 80 mm and 105 mm of the respective slab thickness. The profiled steel deck used in this experimental study is PEVA45 which has a nominal bare metal thickness of 1.0 mm. The schematic design and cross-sectional area of the slab specimens can be referred in Fig. 2. The number of slab specimens is given in Table 3. For slab specimens based on dry density, the slab thickness was made constant at 125 mm. For slab specimens based on slab thickness, the dry density was maintained at 1800 kg/m^3. As can be seen in Fig. 3, the slab specimens go through an air curing process for 28 days.

Table 2 - Number of cube specimens

Density (kg/m^3)	Curing Age		
	7 days	14 days	28 days
1400	3	3	3
1600	3	3	3
1800	3	3	3

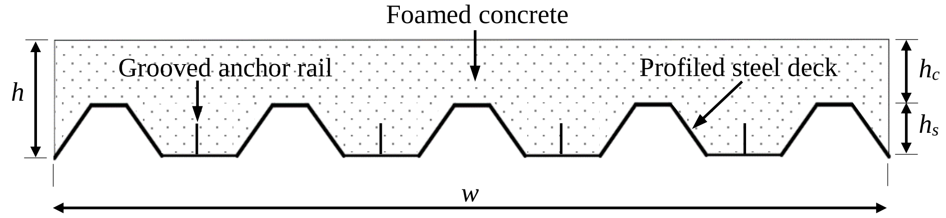

Fig. 2 - Schematic design and cross-sectional area of slab specimens

Table 3 - Number of slab specimens

ID	Dry Density		
	1400 kg/m^3	1600 kg/m^3	1800 kg/m^3
FC1400	3	-	-
FC1600	-	3	-
FC1800	-	-	3
ID	**Slab Thickness**		
	100 mm	**125 mm**	**150 mm**
FCh100	3	-	-
FCh125	-	3	-
FCh150	-	-	3

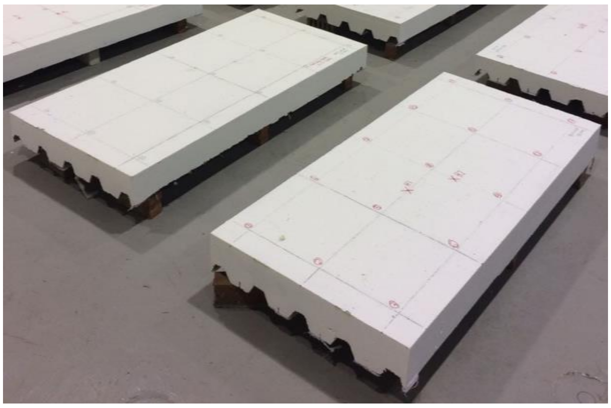

Fig. 3 - Air curing process for slab specimens

3.4 Experimental Tests

There are two types of experimental tests involved in this experimental study. The first is the compression test and the second is the three-point bending test. The compression test was performed on cube specimens to obtain the compressive strength. This was carried out using the ELE Compact Machine 1500 in accordance with BS EN 12390-2 [46]. The applied load is a prescribed rate of 0.14 MPa/minute to 0.34 MPa/minute until the cube specimens are crushed. Before the compression test can be carried out, the cube specimens must be visually inspected, labelled, calibrated and weighted. Usually, slab specimens are subjected to the four-point bending test for flexural strength. It is not common to apply the three-point bending test to the slab specimens. Since this experimental study focuses on the structural behaviour, the three-point bending test has proven to be appropriate. Previous researcher such as Martinez-Martinez [4], Holy et al. [47] and Kita et al. [48] also used the three-point bending test to measure the bending stresses and maximum deflection of slab specimens. The three-point bending test, as shown in Fig. 4, was performed using servo hydraulic static actuator. The load-time history was recorded directly from the load cell, while a linear variable differential transducer (LVDT) was used to measure the deflection-time history.

Fig. 4 - Three-point bending test of slab specimens

4. Results and Discussion

4.1 Compressive Strength

Fig. 5 shows the development of compressive strength during the air curing process. Foamed concrete develops an average of 76.32% compressive strength in the first 7 days, and an additional 16.59% in 14 days. Within 14 days to 28 days, the compressive strength increases by only 7.09%. The development of compressive strength is faster in early age than in later age. For foamed concrete with a density of 1400 kg/m^3, the compressive strength reaches 11.83 MPa in 7 days and increases by up to 14.20 MPa in 14 days. After 28 days of air curing process, the foamed concrete reaches a compressive strength of 15.43 MPa. Zhihua et al. [49] stated that the plain foamed concrete with a density of 1400 kg/m^3 usually has a compressive strength of about 5.7 MPa. A higher compressive strength obtained in this experimental study is attributed to the incorporation of RHA and PMM. The compressive strength of foamed concrete with a density of 1600 kg/m^3 is 17.49 MPa and 20.59 MPa for 7 days and 14 days, respectively. In 28 days, the compressive strength reaches 22.97 MPa which is slightly exceeding the requirements of BS EN 1992-1-1 [11] for load-bearing structures. In the meantime, foamed concrete with a density of 1800 kg/m^3 surpasses the targeted compressive strength. At air curing process of 7, 14 and 28 days, the compressive strength is 25.30 MPa, 29.80 MPa and 32.23, respectively.

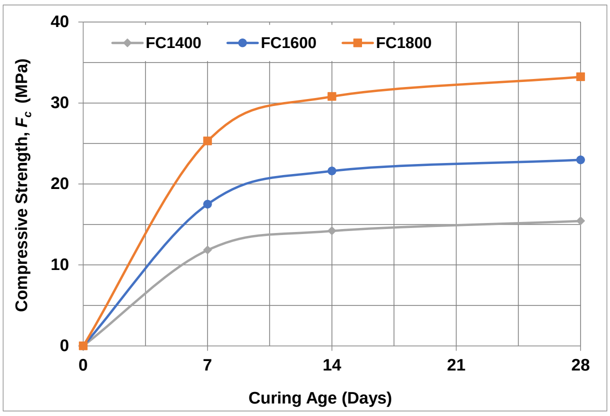

Fig. 5 - Compressive strength foamed concrete in corresponds to curing age

ASTM C330 [12] specifies that lightweight concrete with a density of 1760 kg/m^3 to 1840 kg/m^3 should have a minimum compressive strength of 21 MPa to 28 MPa. Therefore, the foamed concrete produced in this experimental study can be considered suitable for load-bearing structures. The presence of RHA and PMM has an apparent impact on increasing compressive strength. This is because RHA contains pozzolanic substances (predominantly of silica and alumina) that can accelerate the binding time in the early stage of hydration [50]. Isaia et al. [51] found that the reaction of pozzolanic substances and cement in the presence of water exhibits an activity that improves compressive strength. Although PMM has been observed not to have a statistically significant influence on compressive strength, its presence on foamed concrete improves the ability to resist bending stresses and cracks [33]. Another factor affecting compressive strength is dry density. The compressive strength of foamed concrete increases in proportion to its dry density, as can be seen in Fig. 6. According to Hadipramana et al. [52], RHA has the greatest impact on foamed concrete with a dry density greater than 1600 kg/m^3. In contrast, Awang et al. [53] found that PMM has a better contribution to foamed concrete with a dry density lower than 1400 kg/m^3.

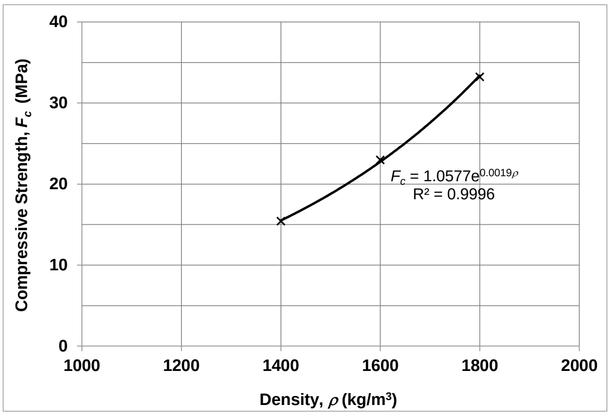

Fig. 6 - The relationship between compressive strength and dry density of foamed concrete

4.2 Ultimate Load and Maximum Deflection

Fig. 7 shows the load-deflection profile of slab specimens subjected to the three-point bending test. The slab specimens, which differ in dry density of foamed concrete, have a pronounced plastic behaviour. A higher dry density tends to achieve a greater ultimate load. This can be attributed to the higher compressive strength accomplished by higher dry density of foamed concrete. The ultimate load of FC1400, FC1600 and FC1800 is 77.46 kN, 85.56 kN and 93.17 kN, respectively. The ultimate load is far higher than that reported by Hulimka et al. [54] on reinforced foamed concrete slabs. The bearing capacity of slab specimens is primarily controlled by profiled steel deck rather than by foamed concrete. However, it must be admitted that the foamed concrete has a paramount function of prolonging the total collapse. Thus, slab specimens can still withstand the applied force in the residual deflection phase. When fracture of foamed concrete occurs, the ultimate load is abruptly reduced and the profiled steel deck solely took over the role of resisting the bending stresses. In this phase, the bearing capacity remains almost constant until the total collapse. In terms of elastic behaviour, FC1600 and FC1800 display a similar linear gradient trend. FC1400 has lower stiffness due to lower compressive strength, resulting in lower modulus of elasticity in foamed concrete.

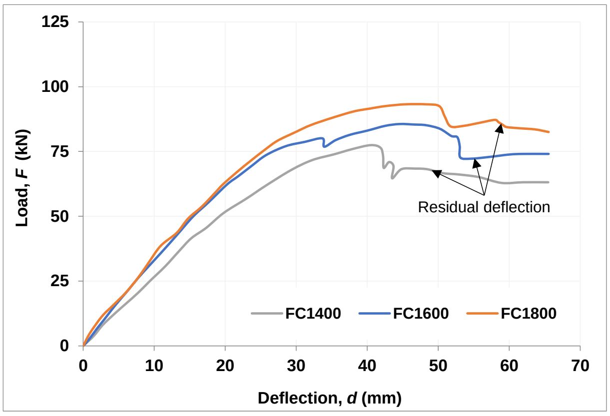

Fig. 7 - Load-deflection profile of FC1400, FC1600 and FC1800

The load-deflection profile of slab specimens with different slab thicknesses is shown in Fig. 8. Despite the different thicknesses, the dry density of foamed concrete is similar at 1800 kg/m^3. Since slab thickness is an important parameter for stiffness, it can be observed that FCh100, FCh125 and FCh1500 have distinct elastic behaviour. A thicker slab thickness tends to have higher stiffness due to the large cross-sectional area and consequently can accommodate an extend of applied force. FCh100 has the ultimate load of 83.25 kN. It is higher than FC1400 with a slab thickness of 125 mm. Although FCh100 has a lower slab thickness than FC1400, the higher dry density reflecting higher compressive strength, means the slab specimens can withstand additional applied force. Meanwhile, the ultimate load of FCh125 and FCh150 is 93.17 MPa and 105.84 MPa, respectively. FCh125 and FC1800 have a similar ultimate load due to the identical characteristics in dry density and slab thickness. Among the slab specimens, FCh150 has the largest ultimate load. In contrast to conventional composite slabs as observed by Hedaoo et al. [55], despite the yielding of profiled steel deck and fracture of foamed concrete, the load drop is not sudden. The ability of foamed concrete to absorb energy allows the slab specimens to sustain the load at residual deflection until total collapse is achieved.

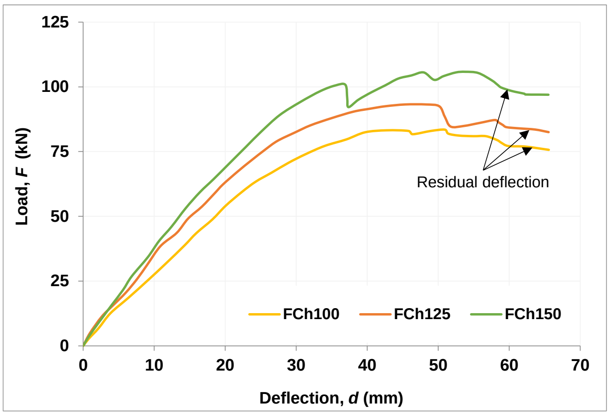

Fig. 8 - Load-deflection profile of FCh100, FCh125 and FCh150

If the ultimate load is plotted according to the dry density and slab thickness, two linear functions can be obtained as shown in Fig. 9. Taking into account these parameters when predicting the ultimate load, the following empirical equation can be formed:

$$F_{ult} = 0.0069\left(0.0197\rho + 0.2080h + 30.0855\right)^{2.0175} \quad (1)$$

where F_{ult} is the ultimate load (in kN), ρ is the dry density of foamed concrete (in kg/m^3) and h is the slab thickness (in mm). Note that this empirical equation is a nondimensionalized version that automatically gives the value of ultimate load in kilonewton. Since compressive strength (*fc*) and span-to-thickness ratio (*L*/*h*) are normally used in the design, an appropriate arrangement to include these two parameters can be made. Known that the dry density of foamed concrete can be depicted as:

$$\rho = 571.6600F_c^{\,0.3277} \quad (2)$$

While the ultimate load in corresponds to span-to-thickness ratio can be written as:

$$F_{ult} = -3.6859\left(\frac{L}{h}\right) + 148.6400 \quad (3)$$

Associating Eq. (2) and Eq. (3) into Eq. (1) establishes the following empirical equation:

$$F_{ult} = 0.0058\left[0.0197\left(517.6600F_c^{\,0.3277}\right) - 1.8430\left(\frac{L}{h}\right) + 85.6030\right]^{2.1339} \quad (4)$$

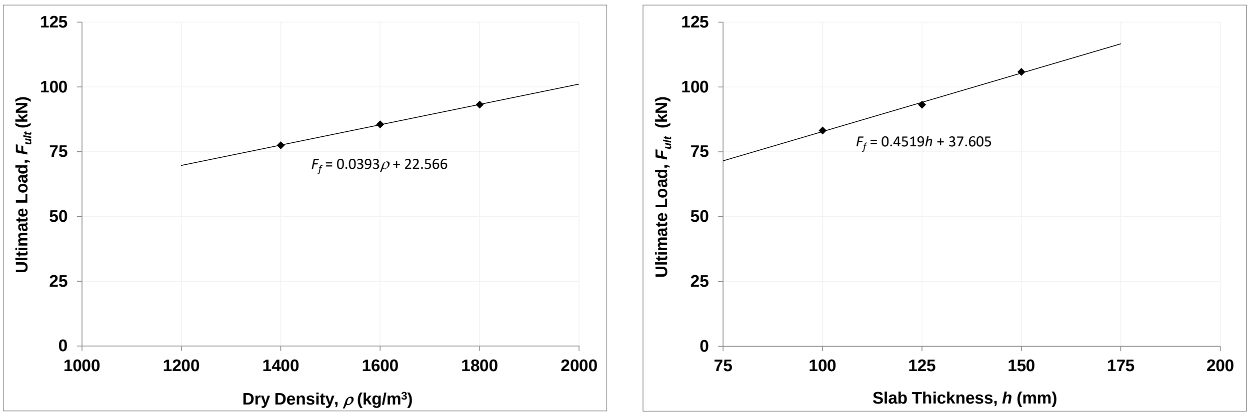

(a) (b)

Fig. 9 - Ultimate load in corresponds to; (a) dry density; (b) slab thickness

Fig. 10 shows the relationship between the maximum deflection with the dry density and the slab thickness. It can be seen that the relationship is about linear trends. Maximum deflection for FC1400, FC1600 and FC1800 is 40.50 mm, 44.58 mm and 48.30 mm, respectively. Meanwhile FCh100, FCh125 and FCh150 have the maximum deflection of 42.76 mm, 48.30 mm and 53.81 mm, respectively. The maximum deflection increases with increasing dry density of foamed concrete by approximately 8.34% to 10.07%. The increase is significant due to the role played by the compressive strength. It is well recognized that as the dry density of foamed concrete increases, its compressive strength eventually increases. Although the influence of compressive strength toward ultimate load is more apparent, but it also contributes to better slip resistance. According to Al-Darzi & Ameer [56], slip resistance is greatly improved by increasing the compressive strength, which allows flexible deformation during the transition to plastic behaviour. With an increase in slab thickness, the maximum deflection increases by 11.41% to 12.96%. If a perfect bond is assumed between the foamed concrete and the profile steel deck, the cross-sectional area governs the structural behaviour in conjunction with the degree of composite action. As the bending stiffness increases with slab thickness, it was found that the higher rate of ductility can be gained by the slab specimens.

Taking the deflection at 75 kN for an instant assessment, FC1400, FC1600 and FC1800 have the deflection of 36.71 mm, 26.91 mm and 25.28 mm, respectively. Meanwhile, FCh100, FCh125 and FCh1500 have the deflection of 32.15 mm, 25.28 mm and 22.24 mm, respectively. This indicates that increasing in dry density and slab thickness contribute to better structural behaviour. In most cases, the deflection of composite slabs is calculated using the average of cracked and uncracked moment of inertia of the cross-sectional area. In this experimental study, no attempt was made to establish the empirical equation for predicting maximum deflection. A typical serviceability criterion of *L*/240 is still relevant for the checking and verifying purposes. It is important to avoid excessive deflection to ensure there are no transient responses, impaired functionality and discomfort. Although the increase in the dry density and slab thickness has cause remarkably increase in the ultimate load, the maximum deflection exceeded the serviceability criterion. Shear bond failure driven by the loss of composite action between the foamed concrete and profiled steel deck was found affecting the measurement of maximum deflection. It should be noted that LVDT was placed on the bottom flange of the profiled steel deck. During the debonding, the maximum deflection is controlled solely by the profiled steel deck.

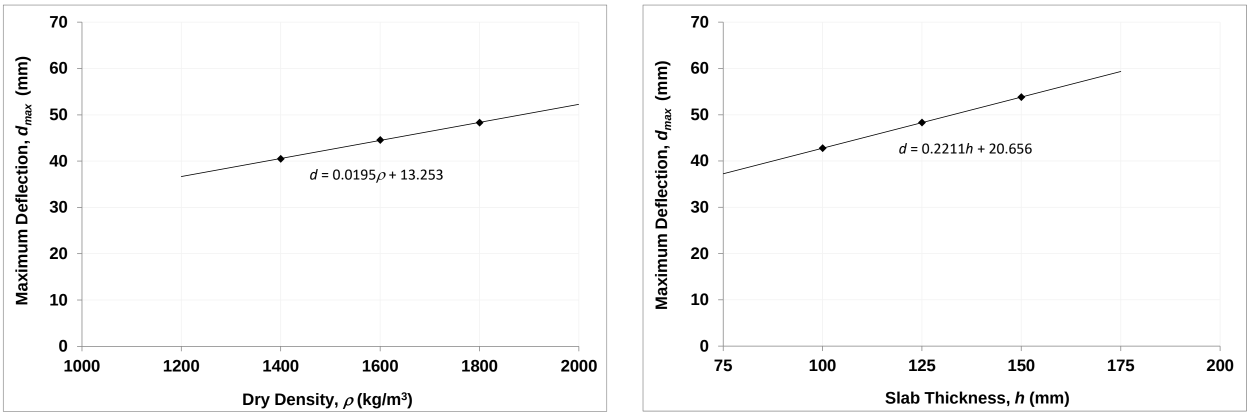

(a) (b)

Fig. 10 - Maximum deflection in corresponds to; (a) dry density; (b) slab thickness

4.3 Failure Mode

Slab specimens exhibited typical failure mode similar to the conventional composite slabs. Localised bending on the profiled steel deck, slip-displacement and fracture of foamed concrete were observed during the experimental study. However, the rate and transition of failure mode differ depending on the physical properties of slab specimens. The onset of yielding occurs much earlier than the ultimate load because the profiled steel deck acts as a tensile reinforcement that carries most of the flexural stresses. The ductile behaviour from the load-deflection profile indicates that the slab specimens are mainly controlled by the profile steel deck rather than the foamed concrete. In Fig. 11, the localised bending was found incurred at the webs along the transverse direction of the profiled steel deck. Meanwhile, fracture of foamed concrete occurs at the free edges of slab specimens. At the phase where the slab specimens experience a large residual deformation, the flexural-shear cracks originating from the interface area cause the slab specimens to total collapse. Because of bending deformation, the longitudinal shear stresses accumulated in the interface area. Since the shear transferring mechanism cannot longer withstand the slip-displacement, the diagonal cracks propagate at the top of the grooved anchor rail. These diagonal cracks can be seen at both ends of slab specimens.

The lack of bond strength between the profiled steel deck and the foamed concrete was the main reason for the shear bond failure. In absence of coarse aggregate, foamed concrete has lower shear strength than normal concrete. Hence, the interface area can be severely damaged if lateral restrain is insufficient. In addition, an irregular development of flexural stresses can cause the shear bond failure related to the horizontal separation between the profiled steel deck and the foamed concrete. This phenomenon was reported by Abbas et al. [3]. Local bond failure occurs when the bond strength is exceeded. When the bond strength completely degraded and the lost reached both ends of the slab specimens, the slippage resulted in total collapse. However, the composite action was not completely lost as the grooved anchor rail acts as a mechanical interlock to transfer the applied force from the foamed concrete to the profiled steel deck. The slab specimens with a lower dry density, especially FC1400, experience large vertical separation inflicted by the foamed concrete overriding. The vertical separation occurs at the top flange and side lap due to the poor mechanical interlock. It principally leads to the reduction of bond strength and contribute to the shear bond failure. This phenomenon is similar to that observed by Abdullah & Easterling [57] on conventional composite slabs.

According to Rackham et al. [2], the bearing capacity of composite slabs is normally dictated by the shear strength rather than by yielding of profiled steel deck. In most cases, the indentations and embossments of the profiled steel deck were found to be effective in magnifying the shear strength and increase the ultimate load [58], [59]. In this experimental study, higher bearing capacity was achieved through higher bending stiffness. For FCh150, the yielding of profiled steel deck occurs prematurely by an indication of a sudden drop in the load-deflection profile. At this phase, the localised bending still invisible and the slab specimens can withstand the increase in applied force largely due to the role of the foamed concrete. Greater slab thickness not only provide higher bending stiffness, but also confirms higher bond strength. This allows the composite action to be fully accomplished and provide sufficient transmitting of longitudinal shear stresses. Previous studies by Jayaseelan et al. [5] and Johnson [60] found that there are obvious effects of slab thickness on the resistance of composite slabs to longitudinal shear stresses and bearing capacity. It was found that FCh150 also demonstrated less slippage between profiled steel deck and foamed concrete. Thus, the diagonal cracks at the tip of the grooved anchor rail are likely to be less intrusive.

(a)

(b)

(c)

Fig. 11 - Failure mode; (a) yielding of corrugated steel deck; (b) flexural-shear cracks; (c) slip-displacement and diagonal cracks

5. Conclusion

This experimental study examines the effects of dry density and slab thickness on the ultimate load, maximum deflection and failure mode of FCCS. It was found that FCSS exhibits a common fashion of ductile behaviour. After yielding of the profiled steel deck, FCCS reaches ultimate load and then fracture of foamed concrete. Overall, FCCS with higher dry density of foamed concrete and higher slab thickness tend to perform better. Due to the higher dry density, excellent bond strength is achieved. The higher dry density attributes to the compressive strength. On the other hand, higher slab thickness contributes to greater bending stiffness, allowing it to withstand a further increase in applied force. The relationship of the load to the dry density and slab thickness is indicated by linear trends. It is similar to the maximum deflection. An empirical equation was established in predicting the ultimate load, considering the dry density and slab thickness as the main parameters. The failure mode of FCCS is similar to the conventional composite slabs. Localized bending in the form of mixed bulging and crippling appears at the webs of profiled steel deck. The shear bond failure causes the slip-displacement. Flexural-shear cracks occur at the free edges of FCCS, while diagonal cracks propagate at the tip of the grooved anchor rail.

Acknowledgement

This experimental study is part of research funded under the Research Acculturation Grant Scheme (Vot. No. R068) and Graduate Research Grant (Vot. No. U696). The authors thank the Ministry of Higher Education and Universiti Tun Hussein Onn Malaysia for financial and spatial support.

References

[1] BS EN 1994-1-1 (2004). Eurocode 4. Design of composite steel and concrete structures - general rules and rules for building. British Standards Institution.

[2] Rackham J. W., Couchman G. H. & Hicks S. J. (2009). Composite slabs and beams using steel decking: Best practise for design and construction. The Steel Construction Institute.

[3] Abbas H. S., Abu Bakar S., Ahmadi M. & Haron Z. (2015). Experimental studies on corrugated steel-concrete composite slab. Gradevinar, 67(3), 225-233.

[4] Martinez-Martinez J. E., Alvarez-Rabanal F. P. & Alonso-Martínez M. (2022). Nonlinear thermos-structural analysis of lightweight concrete and steel decking composite slabs under fire conditions: Numerical and experimental comparison. Applied Sciences, 12, 9306.

[5] Jayaseelan R., Pandulu G. & Mahendran S. (2019). Performance of expanded polystyrene lightweight self-compacting concrete in composite slab. International Journal of Applied Science and Engineering, 18(1), 2019015.

[6] Dian-Zhong L. & Shi-Hao T. (2012). The experimental research on new lightweight steel composite slab. Applied Mechanics and Materials, 188, 157-161.

[7] Lv J., Zhou T., Wu H., Sang L., He Z., Li G. & Li K. (2020). A new composite slab using crushed waste tires as fine aggregate in self-compacting lightweight aggregate concrete. Materials, 13, 2551.

[8] Zhang H. (2011). Building Materials in Civil Engineering. Woodhead Publishing.

[9] Hedjazi, S. (2020). Compressive strength of lightweight concrete. Compressive Strength of Concrete, Pavlo K., IntechOpen.

[10] Chaipanich A. & Chindaprasirt P. (2015). The properties and durability of autoclaved aerated concrete masonry blocks. Eco-efficient Masonry Bricks and Blocks, Pacheco-Torgal F., Lourenco P. B., Labrincha J. A., Kumar S. & Chindaprasirt P., Woodhead Publishing.

[11] BS EN 1992-1-1 (2004). Eurocode 2. Design of concrete structures. General rules and rules for buildings. British Standards Institution.

[12] ASTM C330 (2009). Standard specification for lightweight aggregates for structural concrete. ASTM International.

[13] Hamad A. J. (2017). Size and shape effect of specimen on the compressive strength of HPLWFC reinforced with glass fibre. Journal of King Saud University - Engineering Sciences, 29, 373-380.

[14] Evangelista A. C. J. & Tam V. W. Y. (2020). Properties of high-strength lightweight concrete using manufactured aggregate. Proceeding of the Institution of Civil Engineers - Construction Materials, 173(4), 157-169.

[15] Hung L. V., Tuan N. V. & Thanh L. T. (2021). Experimental investigation of high-strength lightweight concrete using fly ash cenospheres. Lecture Notes in Civil Engineering, 203, 637-645.

[16] Liu H., Elchalakani M., Karrech A., Yehia S. & Yang Bo. (2021). High strength flowable lightweight concrete incorporating low C3A cement, silica fume, stalite and macro-polyfelin polymer fibres. Construction and Building Materials, 281, 122410.

[17] Ibrahim M., Ahmad A., Barry M. S., Alhems L. M. & Suhoothi A. C. M. (2020). Durability of structural lightweight concrete containing expanded perlite aggregate. International Journal of Concrete Structures and Materials, 14, 50.

[18] Lu J. X., Shen P., Ali H. A. & Poon C. S. (2022). Mix design and performance of lightweight ultra high-performance concrete. Materials and Design, 216, 110553.

[19] Pan H., Yan S., Zhao Q. & Wang D. (2022). Preparation and properties of ultra-high performance lightweight concrete. Magazine of Concrete Research, 75(6), 310-323.

[20] Alanazi H., Elalaoui O., Adamu M., Alaswad S. O., Ibrahim Y. E., Abadel A. A. & Al Fuhaid A. F. (2022). Mechanical and microstructural properties of ultra-high performance concrete with lightweight aggregates. Buildings, 12(11), 1783.

[21] Luu T., Bortolotti E., Parmentier B., Kestemont X., Briot M. & Grass J. C. (2009). Experimental investigation of lightweight composite deck slabs. Proceeding of the 9th International Conference on Steel Concrete Composite and Hybrid Structures, Leeds, United Kingdom.

[22] Alvarez Rabanal F. P, Guerrero-Muñoz J. , Alonso-Martinez M. &Martinez-Martinez J. E. (2016). Bending and shear experimental tests and numerical analysis of composite slabs made up of lightweight concrete. Journal of Engineering, 2016, 6819190.

[23] Bruedern A. E., Mechtcherine V., Kurz W. & Jurisch F. (2009). Self-compacting lightweight aggregate concrete for composite slabs. Advances in Cement-Based Materials, Gideon Van Zijl P. A. G. & Boshoff B. P., CRC Press.

[24] Yankun Z., Shaoyu Z. & Xiaoer Z. (2011). Finite element analysis on mechanical properties of lightweight aggregate concrete composite slab. Advanced Materials Research, 250-253, 168-171.

[25] Flores-Johnson E. A. & Li Q. M. (2012). Structural behaviour of composite sandwich panels with plain and fibre-reinforced foamed concrete cores and corrugated steel faces. Composite Structures, 94(5), 1555-1563.

[26] Low J. X., Shek P. N. & Tahir M. M. (2018). Experimental investigation on lightweight composite slab for floating structures. Improving Flood Management, Prediction and Monitoring: Case Studies in Asia, Yusop Z., Aris A., Alias N. E. Annamala K. V. & Waugh W. L., Emerald Group Publishing.

[27] Sutiman N. A., Majid M. A., Jaini Z. M. & Roslan A. S. (2021). Structural behavior of lightweight composite slab system. International Journal of Integrated Engineering, 13(3), 57-65.

[28] Sohel K. M. A., Richard Liew J. Y. & Fares A. I. (2021). Shear bond behavior of composite slabs with ultra-lightweight cementitious composite. Journal of Building Engineering, 44, 103284.

[29] BS EN 1994-1-2 (2015). Eurocode 4. Design of composite steel and concrete structures: General rules - structural fire design. British Standards Institution.
[30] BS EN 12620 (2002). Aggregates for concrete. British Standards Institution.
[31] BS EN 1008 (2002). Mixing water for concrete. Specification for sampling, testing and assessing the suitability of water, including water recovered from processes in the concrete industry, as mixing water for concrete. British Standards Institution.
[32] BS EN 934-2 (2009). Admixtures for concrete, mortar and grout. Concrete admixtures - definitions, requirements, conformity, marking and labelling. British Standard Institute.
[33] Jaini Z. M., Rum R. H. M. & Boon K. H. (2017). Strength and fracture energy of foamed concrete incorporating rice husk ash and polypropylene mega-mesh 55. IOP Conference Series: Materials Science and Engineering, 248, 012005.
[34] Falliano D., De Domenico D., Ricciardi G. & Gugliandolo E. (2018). Key factors affecting the compressive strength of foamed concrete. IOP Conference Series: Materials Science and Engineering, 431, 062009.
[35] Setiono & Gunawana P. (2014). Foamed lightweight concrete tech using galvalum Az 150 fiber. Procedia Engineering, 95, 433-441.
[36] Othman R., Putra Jaya R., Muthusamy K., Sulaiman M. A., Duraisamy Y., Al Bakri Abdullah M. M., Przyby A., Sochacki W., Skrzypczak T., Vizureanu P. & Sandu A. V. (2021). Relation between density and compressive strength of foamed concrete. Materials, 14, 2967.
[37] Al Qubro K., Saggaff A. & Saloma (2021). The compressive strength of fly ash foamed concrete with polypropylene fiber. International Journal of Progressive Sciences and Technologies, 29(1), 447-453.
[38] Ma X., Li C., Chen H., Wei Y., Weng Y. & Li S. (2022). Research on the improving performance of foam concrete applied to the filling of natural gas pipeline cross-river tunnel. Materials, 15, 7461.
[39] Guo Y., Xu C., Hu Z., Wang L., Yue G., Zheng S., Li Q. & Wang P. (2022). Study on the performance of foam concrete prepared from decarburized fly ash. Applied Sciences, 12, 12708.
[40] Abd Rahman N., Khairuddin S. A. A., Faudzi M. F., Mohd Asri M. H. I., Jamaluddin N. & Jaini Z. M. (2020). Axial strength of modified fibrous foamed concrete-filled hollow section. World Journal of Engineering, 17(2), 175-181.
[41] Wong S. H., Shek P. N., Saggaff A., Tahir M. M. & Lee Y. H. (2019). Compressive strength prediction of lightweight foamed concrete with various densities. IOP Conference Series: Materials Science and Engineering, 620, 012043.
[42] Gołaszewski J., Klemczak B., Smolana A., Gołaszewska M., Cygan G., Mankel C., Peralta I., Roser F. & Koenders E. A. B. (2022). Effect of foaming agent, binder and density on the compressive strength and thermal conductivity of ultra-light foam concrete. Buildings, 12, 1176.
[43] Shawnim P. A. & Mohammad F. (2019). Compressive strength of foamed concrete in relation to porosity using SEM images. Journal of Civil Engineering, Science and Technology, 10(1), 34-44.
[44] Chen Y. & Xu Y. F. (2019). Compressive strength of fractal-textured foamed concrete. Fractals, 27, 1940003.
[45] Ouedraogo A. L., Kabre S., Malbila E., Compaore A., Sare R., Ilboudo P., Kam S., Korgo B., Bathiebo D. J., Kieno F. P. & Blanchard P. (2022). Comparative study of the thermal and mechanical properties of foamed concrete with local materials. World Journal of Engineering and Technology, 10, 550-564.
[46] BS EN 12390-2 (2019). Testing hardened concrete. Making and curing specimens for strength tests. British Standards Institution.
[47] Holy M., Citek D., Tej P. & Vrablik L. (2019). Flexural strength of thin slabs made of UHPFRC. Solid State Phenomena, 292, 224-229.
[48] Kita S., Akae S., Sakurai N. & Taniguchi S. (2020). Development of new semi-rigid joint system for slabs (part 2) - verification testing of filler. Nippon Steel Engineering, 11, 46-55.
[49] Zhihua P., Hiromi F. & Tiong H. W. (2007). Preparation of high-performance foamed concrete from cement, sand and mineral admixtures. Journal of Wuhan University of Technology, 22(2), 295-298.
[50] Dembovska L., Bajarea D., Pundieneb I. & Vitolaa L. (2017). Effect of pozzolanic additives on the strength development of high performance concrete. Procedia Engineering, 172, 202-210.
[51] Isaia G. C., Gastaldini A. L. G. & Moraes R. (2003). Physical and pozzolanic action of mineral additions on the mechanical strength of high-performance concrete. Cement and Concrete Composites, 25(1), 69-76.
[52] Hadipramana J., Abdul Samad A. A., Ahmad Zaidi A. M., Mohammad N. & Riza F. V. (2012). Effect of uncontrolled burning rice husk ash in foamed concrete. Advanced Materials Research, 626, 769-775.
[53] Awang H., Mydin M. A. O. & Roslan A. F. (2012). Effects of fibre on drying shrinkage, compressive and flexural strength of lightweight foamed concrete. Advanced Materials Research, 587, 144-149.
[54] Hulimka J., Krzywon R. & Jedrzejewska A. (2017). Laboratory tests of foam concrete slabs reinforced with composite grid. Procedia Engineering, 193, 337-344.
[55] Hedaoo N. A., Gupta L. M. & Ronghe G. N. (2012). Design of composite slabs with profiled steel decking: A comparison between experimental and analytical studies. International Journal of Advanced Structural Engineering, 3, 1-15.

[56] Al-Darzi S. Y. K. & Ameer U. A. (2012). Investigating the effect of concrete strength on the behaviour of composite steel-concrete beams. Journal of Applied Sciences, 12, 2164-2171.
[57] Abdullah R. & Easterling W. S. (2007). determination of composite slab strength using a new elemental test method. Journal of Structural Engineering, 133(9), 1268-1277.
[58] John K., Ashraf M., Weiss M. & Al-Ameri R. (2022). Experimental and finite element study of a novel two-way corrugated steel deck system for composite slabs. Journal of Composites Science, 6, 261.
[59] Avudaiappan S., Saavedra Flores E. I., Araya-Letelier G., Thomas W. J., Raman S. N.,Murali G., Amran M., Karelina M., Fediuk R. & Vatin N. (2021). Experimental investigation on composite deck slab made of cold-formed profiled steel sheeting. Metals, 11, 229.
[60] Johnson R. P. (2015). Designer’s Guide to Eurocode 4: Design of Composite Steel and Concrete Structures. ICE Publishing.